Spatially "chaotic" solutions in reaction-convection models and their bifurcations to moving waves

Olga Nekhamkina and Moshe Sheintuch
Department of Chemical Engineering, Technion—Israel Institute of Technology, Technion City, Haifa 32 000, Israel
(Received 14 June 2001; revised manuscript received 26 March 2002; published 12 July 2002)

The emergence of stationary spatially multiperiodic or even spatially chaotic patterns is analyzed for a simple model of convection, reaction, and conduction in a cross-flow reactor. Spatial patterns emerge much like dynamic temporal patterns in a mixed system of the same kinetics. Moving waves are formed in an unbounded system but they are transformed into stationary spatially inhomogeneous patterns in a bounded system. The sequence of period doubling bifurcations is determined numerically. The incorporation of a slow nondiffusing inhibitor leads to chaotic spatiotemporal patterns.

DOI: 10.1103/PhysRevE.66.016204 PACS number(s): 05.45.−a, 82.40.Bj, 82.40.Ck

I. INTRODUCTION

The increasing interest in reaction-convection-diffusion systems was recently recognized by assigning it a new PACS number (82.40.Ck) that distinguishes it from that of the well studied reaction-diffusion systems. Reaction-convection-diffusion systems are typically described by a system of the form:

$$\mathbf{L}\mathbf{x}_t + \mathbf{V}\mathbf{x}_z - \mathbf{D}\mathbf{x}_{zz} = \mathbf{f}(\mathbf{x}), \tag{1}$$

where $\mathbf{x}$ is the vector of state variables, $\mathbf{L}=\mathrm{diag}\{L_i\}$, $\mathbf{V}=\mathrm{diag}\{V_i\}$, $\mathbf{D}=\mathrm{diag}\{D_i\}$, and L_i, V_i, and D_i are the capacities, velocities, and diffusivities of the various state variables. Reactants can be fed to the reactor either through one port or may be distributed along the reactor via many ports (to which we refer as cross flow). Cross-flow conditions can also be achieved by feeding through a membrane or through a preceding reaction. In the cross-flow reactor we can find a homogeneous solution [$\mathbf{f}(\mathbf{x}_s)=0$]. The technological advantages of such a reactor were argued in Ref. [1].

Stationary pattern formation mechanism in diffusive-reactive systems was suggested in the pioneering work of Turing [2]. The diffusive Turing instability applies to a two-variable system when the inhibitor diffuses sufficiently faster than the activator. This mechanism was able to account for certain patterns in chemistry and biology [3,4], but largely was unable to induce patterns in liquid-phase oscillatory reaction where the reactant diffusivities are usually of similar magnitudes, or in catalytic systems, in which the diffusivity of the activator is typically larger than the diffusivity of the inhibitor.

In the presence of convection a stationary pattern formation mechanism has been recently suggested by Kuznetsov *et al.* [5]. The behavior of spatially distributed system crucially depends on whether the instability is convective or absolute. An instability is called *convective* if a small perturbation induces a local growth from the spatially uniform solution, but disturbances propagate as a wave packet and are advected out of the system. An instability is termed *absolute* if a localized initial perturbation gives rise to growing amplitudes at all points in space. The distinction between absolute and convective instabilities in unbounded systems depends on the choice of the coordinate system and with appropriate transformations to the moving coordinate we can convert one instability to another. The problem becomes definite if we consider a bounded (or semibounded) system with a boundary condition that is fixed at one end. Perturbations applied at the boundary can either penetrate the system, which then acts as a nonlinear filter and a spatial amplifier, or be damped. The pattern-formation mechanism suggested in Ref. [5] is based on the amplification of the stationary perturbations in the convectively unstable systems. Such perturbations can be introduced by the stationary boundary conditions that differ from the steady state solution. This mechanism accounts for stationary patterns in several recent studies: "flow distributed oscillations" (FDO) were extensively investigated in Ref. [6] for the Brusselator model, in Ref. [7] for a Gray-Scott kinetics, in Ref. [8] for the CDIMA reaction, and in Ref. [9] for the Oregonator models and in our previous studies of cross-flow reactors [10–12] with a single Arrhenius first order reaction.

The mechanisms above can also be classified according to the activator/inhibitor parameter ratios, V_1/V_2, D_1/D_2, and L_1/L_2, which define the emergence of stationary patterns. In the FDO stationary patterns emerge even when $D_1=D_2$ [6,8] and it is claimed therefore that these patterns are not due to the Turing mechanism. Diffusion is important for the stationarity of these patterns and the stationary solution breaks down with $D_2=0$. In recent works [10,11] we showed that stationary spatially periodic patterns emerge in a bounded system even when $D_2=0$ provided that the activator capacity L_1 is sufficiently large (for catalytic nonisothermal systems x_1 is typically the temperature and the heat capacity is large, $L_1 \gg 1$).

Other studies have focused on spatiotemporal patterns of Eq. (1). Most notably the well studied differential flow induced chemical instability mechanism [13,14] is connected with the separation of variables due to different convection rates ($V_1 < V_2$).

The studies above were devoted to formation of stationary and moving spatially period-one patterns. In this work we present a general approach for designing stationary patterns of desired complexity. The steady state solutions of the system (1) are governed by a system of ordinary differential equations (ODEs) written in the dimensionless form as $\mathbf{x}_z - \mathbf{P}\mathbf{x}_{zz} = \mathbf{F}(\mathbf{x})$, where $\mathbf{P}=\mathrm{diag}\{\mathrm{Pe}_i^{-1}, \mathrm{Pe}_i = LV_i/D_i\}$, and L is the reactor length. In the limit case $\mathrm{Pe}_i \to \infty$ the spatially

periodic solutions $[\mathbf{x}_z=\mathbf{F}(\mathbf{x})]$ can be predicted from known similar solutions of the temporal behavior of a mixed system governed by the same kinetics $[\mathbf{x}_t=\mathbf{F}(\mathbf{x})]$. We can construct spatially chaotic steady patterns using kinetics known to exhibit temporal chaos. Let the dynamic system exhibit a sequence of period-doubling bifurcations with a varying parameter at $p=p_1,p_2,\ldots,p_n$. Then for the spatially distributed system with $p=p_n$ and other fixed parameters we can expect to find spatially 2^n-periodic solution in the limit case $\mathrm{Pe}_i\to\infty$. For finite Pe_i we expect to find a sequence of bifurcations with increasing Pe from Pe_0 to ∞, where Pe_0 is the bifurcation point to a period-one solution that can be determined by linear analysis (see Ref. [10]). The solution is stable for a sufficiently large L_1. The behavior at finite Pe and the stability of the stationary solutions cannot be predicted by a simple transformation of temporal and spatial coordinates since the system is bounded.

In the present work we demonstrate the mechanism of multiperiodic pattern formation for a model of a catalytic cross-flow reactor with two consecutive reactions governed by three state variables using parameters that are known to yield chaotic temporal behavior in the system $\mathbf{x}_t=\mathbf{f}(\mathbf{x})$ [15].

While oscillatory temporal kinetics is not necessary for obtaining stationary patterns, we also consider the fourth-order system formed by the system above coupled with a slow nondiffusive inhibitor $L_4x_{4,t}=f_4(\mathbf{x})$ in a domain where $\mathbf{L}\mathbf{x}_t=\mathbf{f}(\mathbf{x})$ undergoes the Hopf bifurcation.

II. MATHEMATICAL MODEL

As stated we consider the pseudohomogeneous one-dimensional model of a catalytic cross-flow reactor with two consecutive reactions $A\to B\to C$. The appropriate mathematical model may be written in the following dimensionless form:

$$\mathrm{Le}\frac{\partial y}{\partial\tau}+\frac{\partial y}{\partial\xi}-\frac{1}{\mathrm{Pe}}\frac{\partial^2 y}{\partial\xi^2}=B_1r_1+B_2r_2-S_T=h(x_1,x_2,y,\phi),$$

$$\frac{\partial x_1}{\partial\tau}+\frac{\partial x_1}{\partial\xi}=-r_1-S_{C_1}=f(x_1,y,\phi), \tag{2}$$

$$\frac{\partial x_2}{\partial\tau}+\frac{\partial x_2}{\partial\xi}=r_1-r_2-S_{C_2}=g(x_1,x_2,y,\phi),$$

$$\xi=0,\quad x_i=x_{i,in},\quad y=y_{in};\qquad \xi=\tilde{L},\quad \frac{\partial y}{\partial\xi}=0. \tag{3}$$

Here x_i $(i=1,2)$ and y are dimensionless concentrations and temperature, $r_i(x_i,y,\phi)=\mathrm{Da}_i\phi x_i\exp(y)$ are the chemical reaction rates for very large activation energies and first-order kinetics (Da_i are the Damkohler numbers and ϕ is the reversible catalytic activity), Le is the Lewis number—the ratio of solid- to fluid-phase heat capacities, and $S_{C_i}=\alpha_C(x_i-x_{i,w})$ and $S_T=\alpha_T(y-y_w)$ are mass supply through the wall and heat loss due to cooling. Other notations are conventional. Note, that we used an arbitrary value z_0 as the length scale so that the reactor length $\tilde{L}=L/z_0$ can be varied as a free parameter.

While there is no general agreement on the source and form of activation-deactivation steps, we adopt here a simple linear expression (see Ref. [16]),

$$K_\phi\frac{\partial\phi}{\partial\tau}=a_\phi-b_\phi\phi-y=q(y,\phi), \tag{4}$$

and typically set $K_\phi\gg 1$.

III. ANALYSIS AND SIMULATIONS

We divide the analysis into a constant activity case ($\phi=1$) and a varying activity case. For each case we analyze the system behavior by linear analysis and verify the results with simulations.

A. Constant activity case

Let us review the behavior of several simplified and related systems:

(a) If we ignore the heat-dispersion term then the steady state system

$$\frac{dx_1}{d\xi}=f(x_1,x_2,y,1)=f_1,\quad \frac{dx_2}{d\xi}=g_1,\quad \frac{dy}{d\xi}=h_1 \tag{5}$$

is exactly the model describing the temporal dynamics of a mixed reactor (with ξ replaced by τ). Temporally chaotic solutions are known to exist for this model.

(b) With incorporation of the dispersion term the system may be written as

$$\frac{dx_1}{d\xi}=f_1,\quad \frac{dx_2}{d\xi}=g_1,\quad \frac{dy}{d\xi}=p,\quad \frac{dp}{d\xi}=\mathrm{Pe}(p-h_1). \tag{6}$$

The asymptotic solutions of this system are identical to those of Eq. (5) but the new term affects the stability. The Jacobian matrix of the linearized system (6) is

$$\mathbf{J}=\begin{pmatrix} f_{1_{x_1}} & 0 & f_{1_y} & 0\\ g_{1_{x_1}} & g_{1_{x_2}} & g_{1_y} & 0\\ 0 & 0 & 0 & 1\\ -\mathrm{Pe}h_{1_{x_1}} & -\mathrm{Pe}h_{1_{x_2}} & -\mathrm{Pe}h_{1_y} & \mathrm{Pe}\end{pmatrix}, \tag{7}$$

and the characteristic equation of the eigenvalues (m_j) is the fourth-order polynomial:

$$\det(\mathbf{J}-m\mathbf{I})=\sum_{i=0}^{4}a_im^i=0, \tag{8}$$

with $a_i=a_{i,0}+a_{i,1}\mathrm{Pe}$. The bifurcation to a periodic solution $(m=ik_0)$ occurs at $\mathrm{Pe}=\mathrm{Pe}_0$ that satisfies

$$a\mathrm{Pe}_0^2+b\mathrm{Pe}_0+c=0, \tag{9}$$

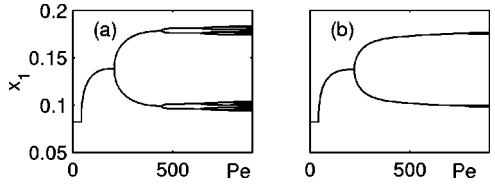

FIG. 1. Bifurcation diagram of system (6) showing period-doubling transitions. (a) $\phi=1$, system convergence to chaos, period-16 solution was obtained at Pe$=780$, and the sequence was not traced further; (b) varying ϕ, $a_\phi=100$ ending with the P_4 solution; $\alpha_T=9$, $\mathrm{Da}_1=0.26$, $\mathrm{Da}_2=0.13$, $B_1=57.77$, and $B_2=-24.61$; computed by AUTO [18].

with $k_0^2=a_1/a_3$. The derivation of Eq. (9) will be presented elsewhere.

(c) We can conduct a linear stability analysis of unbounded system (2) in an infinitely long region. Denoting the deviation from the basic steady state solution $\mathbf{u}_0=\{x_{1s},x_{2s},y_s\}$ as $\mathbf{u}_1=\{x_1,x_2,y_1\}$, and assuming $\mathbf{u}_1\sim e^{ik\xi+\sigma\tau}$, we can derive the dispersion relation $\mathcal{D}(\sigma,k)=0$. The bifurcation condition $\mathrm{Re}(\sigma)=0$ defines the neutral curve, which may be calculated numerically. We used Pe as the bifurcation parameter as it does not influence the steady state solutions and as we intend to employ the results obtained in the limit $\mathrm{Pe}\to\infty$. The neutral curve typically acquires a minimum corresponding to the convective instability threshold (Pe_c, k_c) and crossing Pe_c corresponds to an excitation of waves traveling with a finite k and a constant speed. In a bounded system above $\mathrm{Pe}=\mathrm{Pe}_0$ the waves are transformed into *stationary patterns* (see Refs. [5–10]). For such patterns to emerge, we impose a condition of zero frequency $\omega=0$ in addition to the relation $\mathrm{Re}(\sigma)=0$. If both of these conditions are matched, we may determine a threshold value for amplification of the stationary perturbation. Its coordinates correspond to the Hopf bifurcation point for Eq. (6), defined by Eq. (9), but k_0 is now the spatial wave number.

We chose for our study the set of parameters used in Ref. [17] for exothermic-endothermic consecutive reactions in a mixed reactor since its domain of multiperiodic and chaotic solutions is relatively wide, and the corresponding critical parameters (Pe_0 and the period $T_0=2\pi/k_0$) allow us to suggest observations of these motions in a distributed system with physically reasonable L and Pe values. According to the bifurcation analysis conducted in Ref. [17], increasing α_T yields a Hopf bifurcation at $\alpha_T=8.9408$ followed by a sequence of period-doubling bifurcations that converge to chaotic solutions that exist for $8.965<\alpha_T<9.041$. (To be consistent with that study, we set $\alpha_T=\delta+1$, $x_{1,w}=1$, $x_{2,w}=0$, $y_w=0$.)

The bifurcation diagrams of the ODE system (6) show that, as expected, the homogeneous solutions become unstable at $\mathrm{Pe}=\mathrm{Pe}_0$ [Eq. (9)] and increasing Pe leads to sequences of period-doubling bifurcations that form spatially oscillatory solutions of the same type as the related mixed reactor (see Fig. 1).

Numerical simulations of systems (2) and (3) in the bounded domain ($\tilde{L}=10$) revealed that there exists a steady solution that is transformed with increasing Pe in a way that

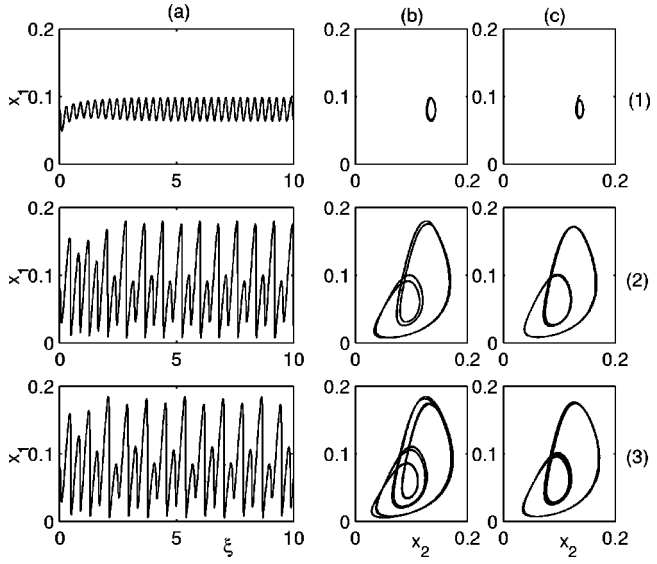

FIG. 2. Bifurcation of spatial patterns in a bounded system for Pe$=45$ (row 1), 500 (row 2), and 1000 (row 3) showing the spatial pattern [column (a), $\phi=1$] and "spatial" phase planes with $\phi=1$ [column (b)] or varying ϕ [$a_\phi=100$, column (c)]; (other parameters as in Fig. 1, Le$=100$).

follows the bifurcation diagrams of the ODE system (6). Below Pe_0 the homogeneous solution is established practically in the whole domain with some adjustment in the inlet section due to the boundary conditions ($x_{i,in}$, y_{in} were adjusted to shorten this inlet effect). Just above the critical values the system exhibits stationary spatial period-one (P_1) patterns [Fig. 2(a), row 1]. The regular single-loop structure is clearly seen in the "spatial" phase planes constructed by plotting $x_1(\xi)$ vs $x_2(\xi)$ profiles from the data in $0.25\tilde{L}<\xi\leqslant\tilde{L}$ [Fig. 2(b), row 1]. The difference between the "numerical" and exact values of k_0 is about 0.1%. With increasing Pe numerical simulations reveal a sequence of period-doubling bifurcations [a period-four solution is shown for Pe$=500$, Figs. 2(a) and 2(b), row 2]. The exact classification of patterns for high Pe is dubious due to the finite size of the

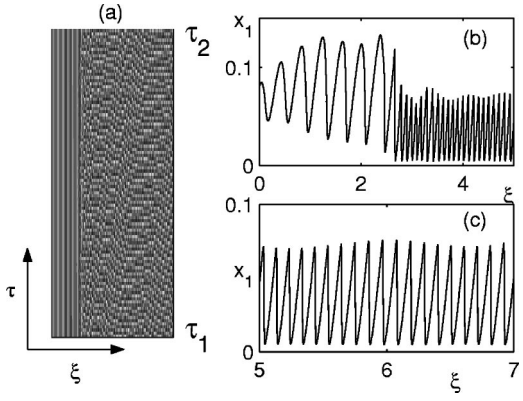

FIG. 3. Spatiotemporal patterns in the varying ϕ case: x_1 is plotted in (a) using a gray scale; (b),(c) fragments of the $x_1(\xi)$ profile at $\tau=\tau_1$; $\alpha_T=9$, $\alpha_\phi=10$, Pe$=1000$, and $K_\phi=5000$.

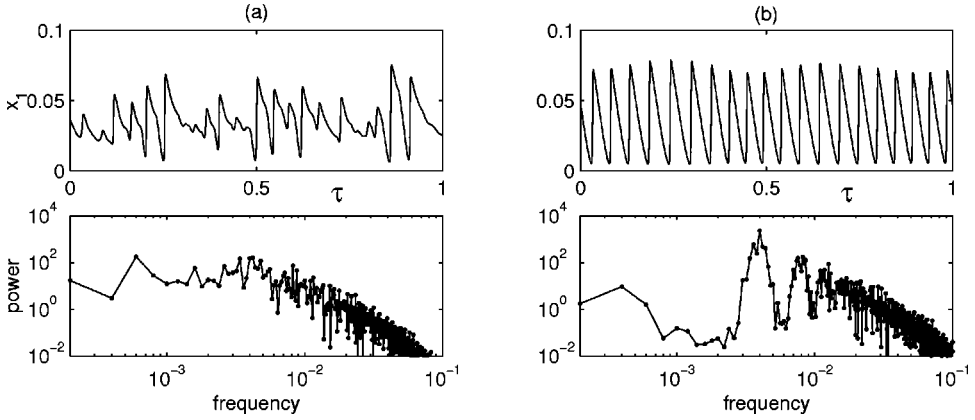

FIG. 4. The temporal profiles of the concentration x_1 and its spectrum at $\xi=0.25\tilde{L}$ (a) and $\xi=0.5\tilde{L}$ (b).

system (for Pe$=700$ a period-eight pattern is expected with a period $T_8=3.234$, so that obviously $\tilde{L}=10$ is not sufficiently long for period recognition). For this reason we cannot claim that the patterns converge into a fully chaotic solution. Yet we note that stationary solutions become practically insensitive to Pe for large Pe [Figs. 2(a) and 2(b), row 3] and coincide with corresponding solutions of the mixed system with fixed initial conditions.

Numerical simulations were conducted by an implicit finite-difference scheme based on the method of fractional steps with 40 000 spatial grid points.

B. The variable catalytic activity case

We repeat the steady state analysis presented above by adding the algebraic relation

$$\phi=\frac{a_\phi-y}{b_\phi} \tag{10}$$

to system (6). The critical parameters Pe_0, k_0 can be determined from Eq. (9) as well, using the gain differentiating rule for functions f,g,h while accounting for Eq. (10). To simplify the following analysis we used a_ϕ as a free parameter and defined $b_\phi=a_\phi-y_s$ in order to ensure that changes in a_ϕ do not affect the steady state solution $(x_{1s}, x_{2s}, y_s, 1)$. Obviously as $a_\phi\to\infty$, $\phi\to 1$. For very large a_ϕ the bifurcation diagrams preserve the same form as for the constant activity case. With decreasing a_ϕ the number of period-doubling transitions in the domain $\mathrm{Pe}_0<\mathrm{Pe}<\infty$ decreases. (Thus, for $\alpha_T=9.0$ and $a_\phi=1000$ we still find a spatially chaotic behavior, with $a_\phi=100$ the sequence of bifurcations converges to P_4 solution [see Fig. 1(b), and with $a_\phi=10$ a period-one solution is stable for all $\mathrm{Pe}>\mathrm{Pe}_0$].

We start now to study the dynamics. For sufficiently high a_ϕ and moderate K_ϕ the system is stable and its behavior is quite similar to the case $\phi=1$ [see Fig. 2(c)]. The effect of decreasing a_ϕ or increasing K_ϕ is to destabilize the system by inducing a front motion as in a typical activator-inhibitor system. ϕ is the slow variable and its response is more sluggish as K_ϕ increases. Beyond a certain threshold, determination of which is out of the scope of this paper, the system undergoes a transition to spatiotemporal motion; Fig. 3 ($\alpha_T=9$, $a_\phi=10$; the analysis predicts a simple period-one solution for $\mathrm{Pe}>\mathrm{Pe}_0=74.8$) presents a pattern composed of several stationary waves near the inlet and a rather aperiodic wave packet that moves upstream. The aperiodic nature of the spatial signal was verified from its power spectra (not presented) showing several leading frequencies. With increasing Pe or K_ϕ the width of the stationary wave packet diminishes while the moving packet broadens.

In the power spectrum of the temporal signal around the boundary between the stationary and moving waves (here at $\xi=0.25\tilde{L}$) we cannot distinguish any leading frequency [Fig. 4(a)].

The solution becomes more regular with increasing ξ [Figs. 4(b) and 4(c)]. With increasing Pe and/or K_ϕ the spectral characteristics become more complicated. Similar results were obtained for smaller α_T, but the region where stable stationary patterns exist is shifted to a range of larger Pe and K_ϕ values.

IV. CONCLUSIONS

Finally we comment about the interaction of the system length $\tilde{L}$ and the period of oscillations T. We observed stationary period-one, period-two or period-four patterns, and we can expect the emergence of more complicated structures with increasing $\tilde{L}$. On the other hand the effect of the inlet boundary conditions cannot propagate for an infinitely long distance and this case requires further study.

To summarize our results, we presented a mechanism for the emergence of spatially chaotic or spatially multiperiodic stationary patterns in a convection-diffusion-reaction system and demonstrated it on a system with two consecutive reactions in a cross-flow reactor. The results apply to any system of the form of Eq. (1) when its ODE analog, $\mathbf{x}_t=\mathbf{f}$, exhibits temporally chaotic solutions. The interaction of this system with a slow, nondiffusing, and localized inhibitor may lead to spatiotemporal patterns.

ACKNOWLEDGMENTS

This work was supported by the Volkswagen-Stiftung Foundation. M.S. acknowledges the Minerva Center of Nonlinear Dynamics for support. O.N. was partially supported by the Center for Absorption in Science, Ministry of Immigrant Absorption, State of Israel.

[1] K.R. Westerterp, W.P.M. Van Swaaij, and A.A.C.M. Beenackers, *Chemical Reactor Design and Operation* (Wiley, New York, 1984).
[2] A.M. Turing, Philos Trans. R. Soc. London Ser. B, **237**, 37 (1952).
[3] A. De Wit, Adv. Chem. Phys. **109**, 435 (1999).
[4] J.D. Murray, *Mathematical Biology* (Springer-Verlag, Berlin, 1993).
[5] S.P. Kuznetsov, E. Mosekilde, G. Dewel, and P. Borckmans, J. Chem. Phys. **106**, 7609 (1997).
[6] P. Andresén, M. Bache, E. Mosekilde, G. Dewel, and P. Borckmanns, Phys. Rev. E **60**, 297 (1999).
[7] R.A. Satnoianu and M. Menzinger, Phys. Rev. E **62**, 113 (2000).
[8] J.R. Bamforth, S. Kalliadasis, J.H. Merkin, and S.K. Scott, Phys. Chem. Chem. Phys. **2**, 4013 (2000).
[9] J.R. Bamforth, J.H. Merkin, S.K. Scott, R. Tóth, and V. Gáspár, Phys. Chem. Chem. Phys. **3**, 1435 (2001).
[10] O.A. Nekhamkina, A.A. Nepomnyashchy, B.Y. Rubinstein, and M. Sheintuch, Phys. Rev. E **61**, 2436 (2000).
[11] O.A. Nekhamkina, B.Y. Rubinstein, and M. Sheintuch, AIChE J. **46**, 1632 (2000).
[12] O.A. Nekhamkina, B.Y. Rubinstein, and M. Sheintuch, Chem. Eng. Sci. **56**, 771 (2001).
[13] A.B. Rovinsky and M. Menzinger, Phys. Rev. Lett. **69**, 1193 (1992).
[14] V.Z. Yakhnin, A.B. Rovinsky, and M. Menzinger, Chem. Eng. Sci. **49**, 3257 (1994).
[15] D.V. Jorgensen and R. Aris, Chem. Eng. Sci. **38**, 45 (1983).
[16] M. Barto and M. Sheintuch, AIChE J. **40**, 120 (1994).
[17] R.M. Chemburkar, O.E. Rössler, and A. Varma, Chem. Eng. Sci. **42**, 1507 (1987).
[18] E.J. Doedel, Congr. Numer. **30**, 265 (1981).